scientific reports

Check for updates

OPEN

# Quantitative ultrasound classification of healthy and chemically degraded ex-vivo cartilage

Angela Sorriento[1,2]✉, Lorena Guachi-Guachi[1,2], Claudia Turini[1,2], Enrico Lenzi[3], Paolo Dolzani[3], Gina Lisignoli[3], Sajedeh Kerdegari[4,5], Gaetano Valenza[6,7], Claudio Canale[4], Leonardo Ricotti[1,2] & Andrea Cafarelli[1,2]

**In this study, we explore the potential of ten quantitative (radiofrequency-based) ultrasound parameters to assess the progressive loss of collagen and proteoglycans, mimicking an osteoarthritis condition in ex-vivo bovine cartilage samples. Most analyzed metrics showed significant changes as the degradation progressed, especially with collagenase treatment. We propose for the first time a combination of these ultrasound parameters through machine learning models aimed at automatically identifying healthy and degraded cartilage samples. The random forest model showed good performance in distinguishing healthy cartilage from trypsin-treated samples, with an accuracy of 60%. The support vector machine demonstrated excellent accuracy (96%) in differentiating healthy cartilage from collagenase-degraded samples. Histological and mechanical analyses further confirmed these findings, with collagenase having a more pronounced impact on both mechanical and histological properties, compared to trypsin. These metrics were obtained using an ultrasound probe having a transmission frequency of 15 MHz, typically used for the diagnosis of musculoskeletal diseases, enabling a fully non-invasive procedure without requiring arthroscopic probes. As a perspective, the proposed quantitative ultrasound assessment has the potential to become a new standard for monitoring cartilage health, enabling the early detection of cartilage pathologies and timely interventions.**

The unique properties of articular cartilage are closely linked to the composition and structure of the extracellular matrix, which is mainly composed of a high concentration of proteoglycans (particularly aggrecan), included in a dense network of collagen fibers and water. Proteoglycans endow cartilage tissue with resilience and elasticity, while the collagen network determines its shape and tensile stiffness[1]. Articular cartilage degeneration can occur, due to thraumas or age. Cartilage degeneration is a condition that affects millions of people globally, resulting in pain and functional impairment[2] It leads to long-term complications in the most severe cases, such as the onset of osteoarthritis (OA)[3]. Nowadays, the management of articular cartilage degeneration is still an open issue. In addition to novel treatments, there is also a need for more sensitive and quantitative methods to facilitate early detection of cartilage lesions, as well as to assess treatment outcomes reliably[4]. Current diagnostic techniques, such as physical examinations, symptom assessments, and conventional radiographs, often suffer from subjectivity, susceptibility to errors, or radiation exposure. Magnetic resonance imaging is a safe and accurate technique for OA diagnosis; however, it is not routinely used as it is expensive and time-consuming. Ultrasound (US) offers a promising and safe alternative for cartilage monitoring[5]. However, conventional B-mode imaging examinations primarily provide qualitative and subjective morphological information. An exciting perspective is given by quantitative ultrasound (QUS) techniques. They work directly on the raw radiofrequency (RF) data derived

[1]The BioRobotics Institute, Scuola Superiore Sant'Anna, 56127 Pisa, Italy. [2]Department of Excellence in Robotics & AI, Scuola Superiore Sant'Anna, 56127 Pisa, Italy. [3]SC Laboratorio di Immunoreumatologia e Rigenerazione Tissutale, IRCCS Istituto Ortopedico Rizzoli, 40136 Bologna, Italy. [4]Physics Department, University of Genoa, via Dodecaneso 33, 16146 Genoa, Italy. [5]Nanoscopy, Istituto Italiano di Tecnologia, Via Enrico Melen, 83 Edificio B, 16152 Genoa, Italy. [6]Bioengineerring and Robotics Research Centre E Piaggio, University of Pisa, 56122 Pisa, Italy. [7]Department of Information Engineering, University of Pisa, 56123 Pisa, Italy. ✉email: angela.sorriento@santannapisa.it

from the piezoelectric elements of the US probe, and they enable a quantitative and objective characterization of the examined tissues[6].

In the existing literature, QUS methods have been explored for the analysis of various soft tissues, trying to correlate the acquired backscattered US signals with alterations in the content and architecture of the tissues[7]. Concerning cartilage, different studies explored the use of high-frequency US (20 MHz ≤ f ≥ 50 MHz) to distinguish between healthy and degraded cartilage[8–11]. The parameters typically used in these studies include time domain metrics (e.g., speed of sound (SoS), reflection index (RI), surface roughness (URI), and thickness) and frequency domain parameters (e.g., attenuation coefficient, integrated backscatter coefficient (AIB), and integrated reflection coefficient (IRC)). Kaleva et al.[12] compared time-domain, frequency domain, and wavelet transform QUS parameters in terms of their ability to detect degenerative changes in healthy and spontaneously degraded osteochondral samples of bovine patellae, using a transmission frequency equal to 20 MHz. Their results demonstrated that all the analyzed acoustic parameters were capable of detecting degenerative signs; time-domain parameters resulted as sensitive and specific as the more complex frequency-domain or wavelet parameters. Interesting findings were also observed in ex-vivo naturally degraded human articular cartilage[13]. The authors used high frequency US (29 MHz) to derive thirteen QUS parameters calculated from the normalized spectrum of the RF signals, and effectively able to detect early OA signs. Similarly, a correlation between acoustic parameters (such as URI and RI) and OA grade was also observed in OA-induced animal models, using high-frequency US at 55 MHz[14]. In the studies described above, the degradation process was spontaneous, while in other works, the process was chemically induced to better control degradation, by regulating the exposure time to enzymes. Among enzymatic degradation solutions, trypsin is commonly used for simulating the proteoglycan loss during cartilage degeneration, while collagenase is used to mimic the degradation of the collagen network. Wang et al.[8] explored high-frequency QUS (40 MHz) to derive URI, AIB, IRC, and other acoustic properties of normal and articular cartilage degraded using trypsin (4 h) and collagenase (24 h). Saarakkala et al.[9], also investigated the use of high-frequency US (20 MHz), in ex-vivo bovine articular cartilage degraded with collagenase (44 h) and trypsin (60 min). The authors found variations in the proposed QUS parameters (RI, URI and spatial variation of US reflection), due to the enzymatic treatments. All the studies described used high-frequency US. This technology guarantees intrinsic high resolution; however its potential use in the clinical practice is limited due to the low in-vivo penetration capability, which makes necessary the use of arthroscopic probes or other relatively invasive procedures. Only a few studies used lower frequencies (< 20 MHz) to detect degenerative changes in the cartilage tissue. Zhang et al.[15] examined the degradation effects induced by trypsin at 2 h and 4 h, using a frequency of 15 MHz. The authors calculated three acoustic parameters (IRC, AIB and averaged magnitude ratio), which were able to detect the loss of proteoglycans. Hattori et al.[16] investigated articular cartilage treated with collagenase at different time points of degradation (1 h, 2 h, 4 h, 8 h, 16 h, 24 h), both in-vivo and in-vitro. They calculated the maximum magnitude and echo duration from the wavelet transformation of the RF signal, noting an increase in the maximum magnitude as the duration of collagenase degradation increased.

It is worth mentioning that this research field is affected by a lack of standardization. Among the mentioned studies, some authors focused only on the effects of trypsin, while others focused on collagenase ones, with degradation time points that vary among different studies. Recently, we proposed a combination of phase sample entropy (sampEn) and amplitude information, to distinguish between various concentrations of bone mineral content in phantoms mimicking the regeneration of the bone after fracture[17]. We also explored the potential of the sampEn parameter, thickness and RI for discriminating healthy cartilage from cartilage treated with trypsin and collagenase at a single degradation time point[18].

To the best of our knowledge, nobody has systematically investigated the correlation between QUS parameters and the effects of the degradation induced by trypsin and collagenase at different time points, using US frequencies that can be used non-invasively in the clinical practice (f < 20 MHz). In this study, we propose, for the first time, a combination of novel quantitative parameters and artificial intelligence (AI) algorithms to automatically discriminate healthy from chemically degraded cartilage. Cartilage samples were obtained from healthy bovine condyles, treated with trypsin and collagenase solutions and analyzed at different time points. Three time points were chosen for the measurements: for the trypsin treatment, t = 0 h (control), t = 2 h (moderate degradation) and t = 4 h (severe degradation) were set; for the collagenase treatment, t = 0 h (control), t = 6 h (moderate degradation) and t = 24 h (severe degradation) were set. RF data were acquired using a transmission frequency of 15 MHz and analyzed offline to derive quantitative diagnostic metrics. Histological evaluations and nanoindentation analyses were performed to confirm the differences found in the different cartilage samples in terms of both structure and mechanical properties.

## Results

### US measurements and data analysis

The values of the ten QUS metrics extracted from the RF signals at the different time-points are shown in Fig. 1 for the trypsin and in Fig. 2 for the collagenase treatment (for further details regarding the metrics calculation, please refer to the appendix section in the supplementary material). The explored QUS metrics were grouped into two distinct sub-datasets: complexity and irregularity and cartilage features (see Materials and Methods section).

*Complexity and irregularity*

In Figs. 1a and 2a, the six metrics indicating the complexity and irregularity of the RF signals are reported: *(i) sample entropy (sampEn)*, *(ii) multiscale entropy* and *(iii) fuzzy entropy* compute the complexity of time series to provide information about the structural integrity of the treated samples, *(iv) fractal dimension* is a measure of complexity in a pattern to describe textural characteristics of the treated samples, *(v) kurtosis* measures data

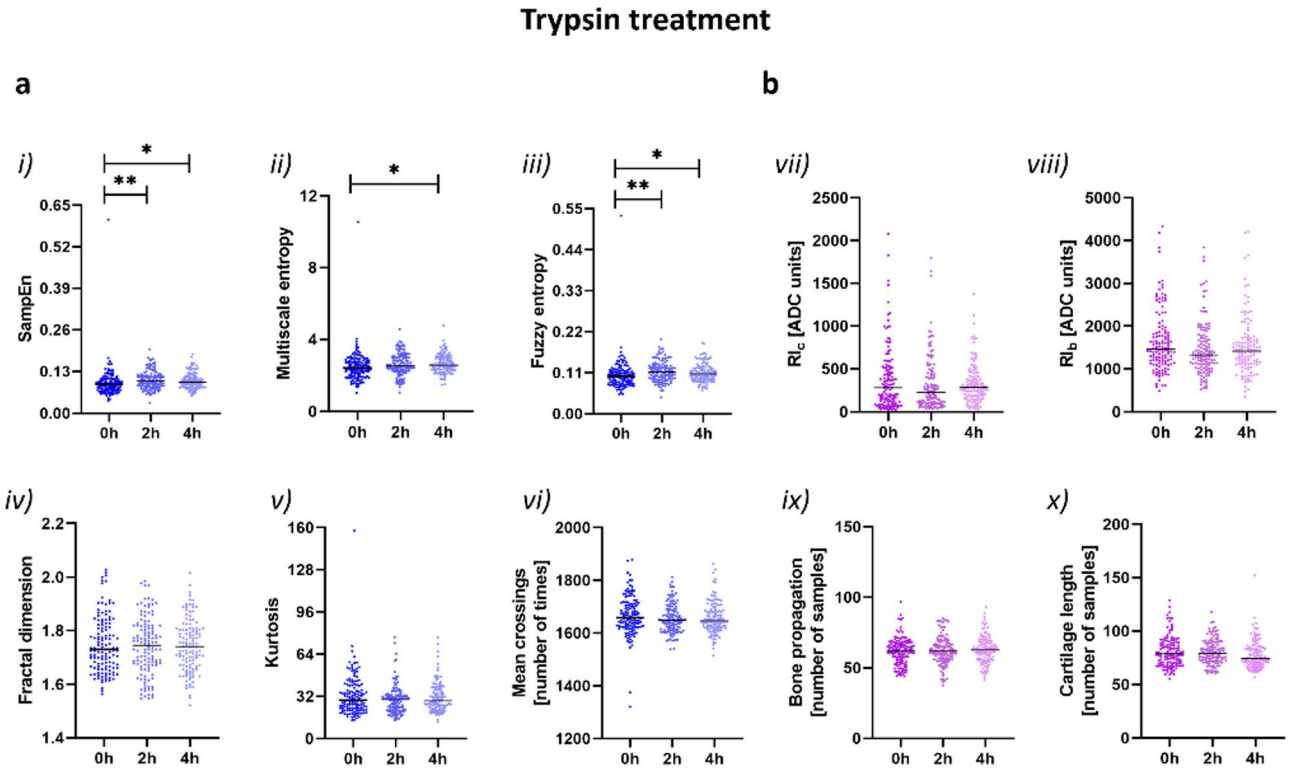


**Fig. 1**. QUS metrics of cartilage samples treated using trypsin. Complexity and irregularity parameters are reported in (**a**) *i) sampEn*, *ii) multiscale entropy*, *iii) fuzzy entropy*, *iv) fractal dimension*, *v) kurtosis*, *vi) mean crossing*. *Multiscale entropy* was derived by computing *sample entropy* across 10 scales, with the area under the resulting curve serving as its measure. Cartilage features are reported in (**b**) *vii)* $RI_c$, *viii)* $RI_b$, *ix) bone propagation*, *x) cartilage length*. Group-wise differences were analyzed using the non-parametric Kruskal-Wallis test, with Dunn's test as a post-hoc analysis for multiple comparisons. $^{*}p<0.0332$, $^{**}p<0.0021$, $^{***}p<0.0002$, $^{****}p<0.0001$. N consisted of 128 independent tissue samples at 0 h, 124 at 2 h and 120 at 4 h, with 21 RF lines analyzed per sample.

distribution in a time series to evaluate regularity properties of the samples, *(vi) mean crossing* counts the number of times a series crosses its mean value to provide information about complexity and textural information of the sample. The parameters associated with entropy measurement (*sampEn*, *multiscale entropy* and *fuzzy entropy*) showed a slight increase after 4 h of trypsin treatment. *SampEn and fuzzy entropy* also exhibited significant changes between 0 h and 2 h of trypsin treatment. Regarding collagenase treatment, most of the analyzed parameters, except *fractal dimension and kurtosis*, exhibited significant differences between 0 h and 24 h. *Multiscale entropy* and *mean crossing* also showed a significant variation between 0 h and 6 h.

*Cartilage features*

In Figs. 1b and 2b, the four parameters closely associated with the cartilage structure, are reported: *vii)* RI at the water-cartilage interface ($RI_c$), *viii)* RI at the cartilage-bone interface ($RI_b$), *ix) bone propagation* calculated as number of samples between the bone interface and the last peak in the RF signal, *x) cartilage length* in terms of the number of samples between the water-cartilage interface and the cartilage-bone interface. All cartilage features were mildly affected by trypsin treatment, with no significant variations observed. $RI_c$ significantly decreased as cartilage degeneration progressed under collagenase treatment, resulting in complete cartilage loss at 24 h. This explains the absence of $RI_c$ measurement at 24 h for collagenase. $RI_b$ showed no change in response to collagenase treatment. The *bone propagation* and *cartilage length* revealed considerable alterations after collagenase treatments at different time points of degradation. In addition, the cartilage thickness can be derived from the *cartilage length* by determining the time of flight and the SoS of healthy cartilage and degraded cartilage (for further details, please refer to the appendix section in the supplementary material). Thickness measurements derived from US analysis, compared with those from histological analysis, are reported in Figure S1 of the supplementary material.

All the results of the QUS parameters in terms of median ± interquartile range are reported in Table S1.

*Machine learning-based classification*

QUS metrics were employed to automatically classify cartilage samples across two and three degradation levels using machine learning (ML) models. Six ML models were evaluated for their effectiveness in distinguishing healthy from degenerated tissue, as well as in differentiating among distinct stages of degradation (healthy,

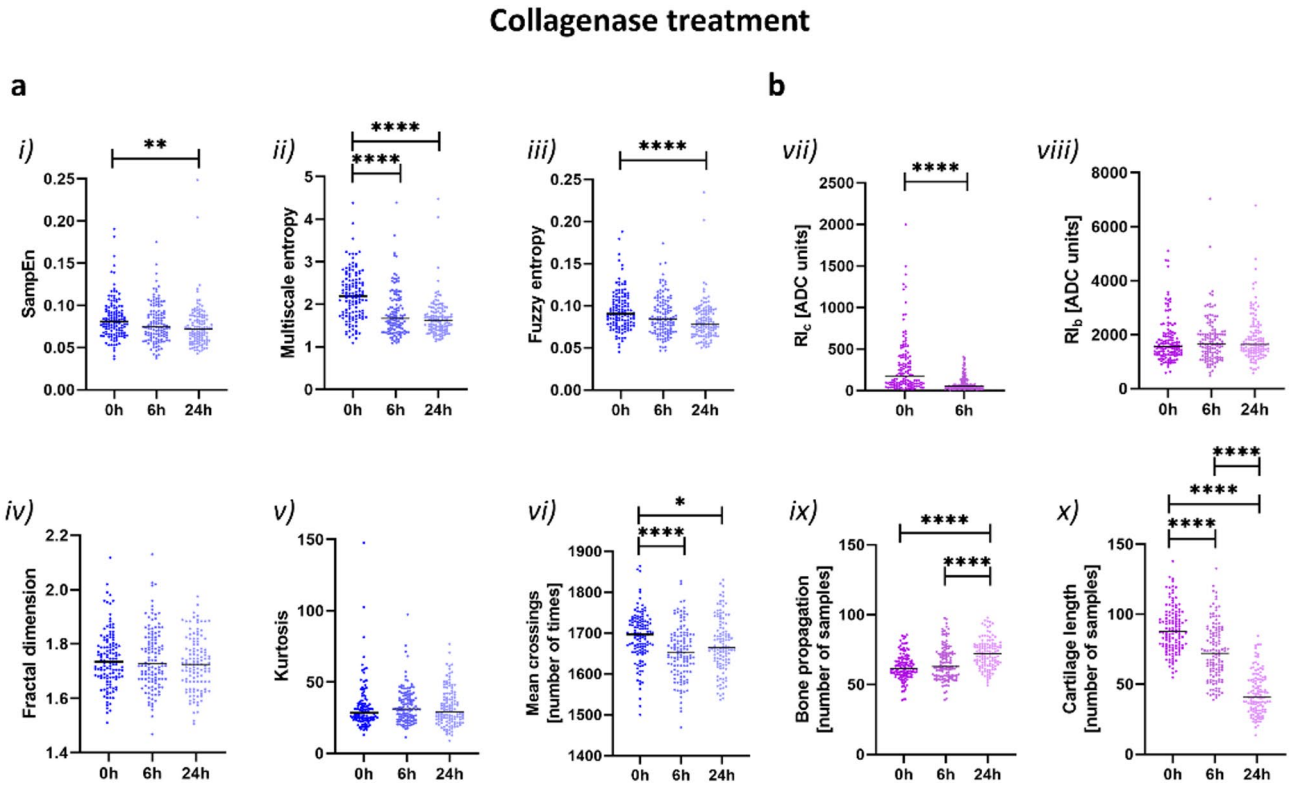


**Fig. 2**. QUS metrics of cartilage samples treated using collagenase. Complexity and irregularity parameters are reported in (**a**): *(i) sampEn*, *(ii) multiscale entropy*, *(iii) fuzzy entropy*, *(iv) fractal dimension*, *(v) kurtosis*, *(vi) mean crossing*. *Multiscale entropy* was derived by computing *sample entropy* across 10 scales, with the area under the resulting curve serving as its measure. Cartilage features are reported in (**b**): *(vii)* $RI_c$, *(viii)* $RI_b$, *(ix) bone propagation*, *(x) cartilage length*. Group-wise differences were analyzed using the non-parametric Kruskal-Wallis test, with Dunn's test as a post-hoc analysis for multiple comparisons. $^{*}p < 0.0332$, $^{**}p < 0.0021$, $^{***}p < 0.0002$, $^{****}p < 0.0001$. N consisted of 126 independent tissue samples at 0 h, 122 at 6 h and 118 at 24 h, with 21 RF lines analyzed per sample.

moderate, and severe) induced by enzymatic treatments. For binary classification, two time points were used per enzyme: 0 h and 4 h for trypsin, and 0 h and 24 h for collagenase. For multiclass classification, three time points were selected: 0 h, 2 h, and 4 h for trypsin, and 0 h, 6 h, and 24 h for collagenase, reflecting progressive tissue degradation. These models were developed and tested using the Leave-One-Out Cross-Validation (LOOCV) technique[19]. Moreover, a feature analysis was conducted to determine the contribution score of each feature in effectively distinguishing samples at each time point (Figure S2 of the supplementary material).

Table S2 and Table S3 summarize the overall performance of the developed ML models in classifying two and three levels of tissue degradation, using both the original QUS dataset and the augmented dataset. The results demonstrated that the models performed effectively in the binary classification task. Specifically, the random forest model achieved the highest accuracy (60%) for trypsin-induced degradation, while the SVM model reached the highest accuracy (96%) in distinguishing between the two classes for collagenase treatment. However, when attempting to classify three levels of degradation, the accuracy decreased to 41% for trypsin (Random Forest) and 71% for collagenase (SVM and Logistic Regression). This reduction indicates that, while effective for binary classification, the dataset may require further enrichment to support reliable multi-level degradation assessment. To improve model performance under these conditions, an augmented dataset was generated using the SMOTE technique. This enrichment led to a significant improvement in classification accuracy, reaching 93% for trypsin and 96% for collagenase using the Random Forest model. A detailed analysis of the confusion matrices for both the two and three class classifications is provided in Fig. 3. When distinguishing between two degradation levels (Fig. 3a), the random forest model applied to trypsin-treated samples exhibited an overall misclassification rate of 40%, with 21% of degenerated samples misclassified as healthy. In contrast, the SVM model applied to collagenase-treated samples achieved an overall misclassification rate of just 3%, with only 0.4% of degenerated samples incorrectly classified. When extending the classification to three degradation levels (Fig. 3b), the random forest model for trypsin treatment achieved an overall misclassification rate of 58%, with 19% of degenerated samples misclassified as healthy. For collagenase-treated samples, the SVM model yielded an overall misclassification rate of 29%, with 7% of degenerated samples incorrectly classified. Notably, when using the augmented dataset (Fig. 3c), both models showed substantial improvements. The random forest model applied to trypsin-treated samples achieved an overall misclassification rate of just 7%, with only 3% of

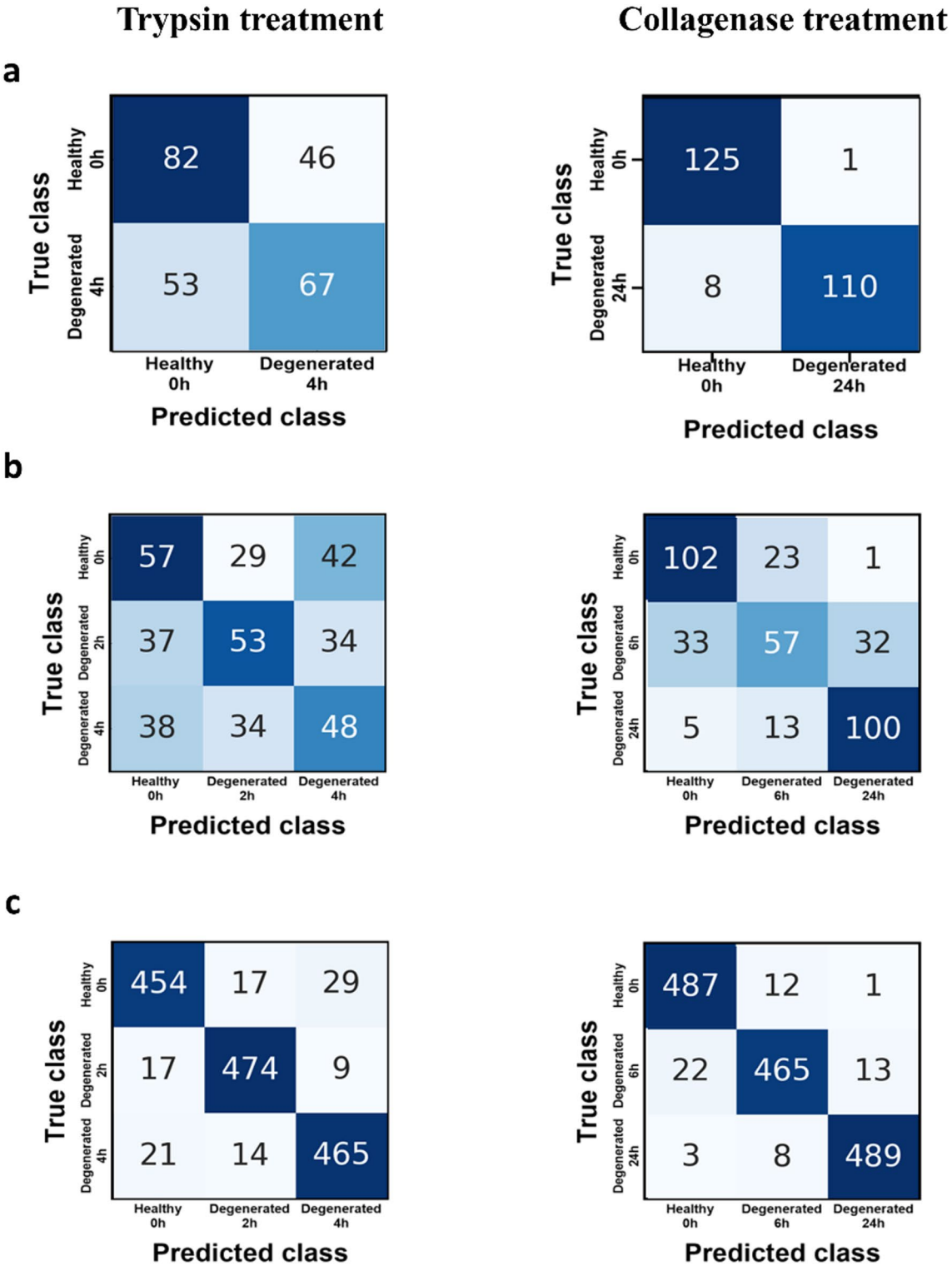


**Fig. 3**. Confusion matrices of the classifiers with the highest accuracy achieved for trypsin and collagenase treatment: (**a**) random forest and SVM to distinguish 2 levels of degradation; (**b**) random forest and SVM to distinguish 3 levels of degradation; (**c**) random forest to distinguish 3 levels of degradation, where a SMOTE technique was applied for generating synthetic samples, creating a dataset with 500 samples per class.

degenerated samples misclassified. Similarly, the random forest model for collagenase treatment reported a 4% overall error rate, with misclassification of degenerated samples reduced to 2%.

## Histological analyses

*Trypsin treatment*

Safranin O positive staining evidenced a progressive and significant decrease in proteoglycan content over time after trypsin treatment (Fig. 4a, b). Before trypsin treatment (0 h), the cartilage area was 100% positive for the staining. After 2 h of treatment (2 h), the positive surface area decreased approximately to 20% of the total cartilage area, and after 4 h (4 h), the positivity dropped almost to 0%. Only in a few cases, we observed a

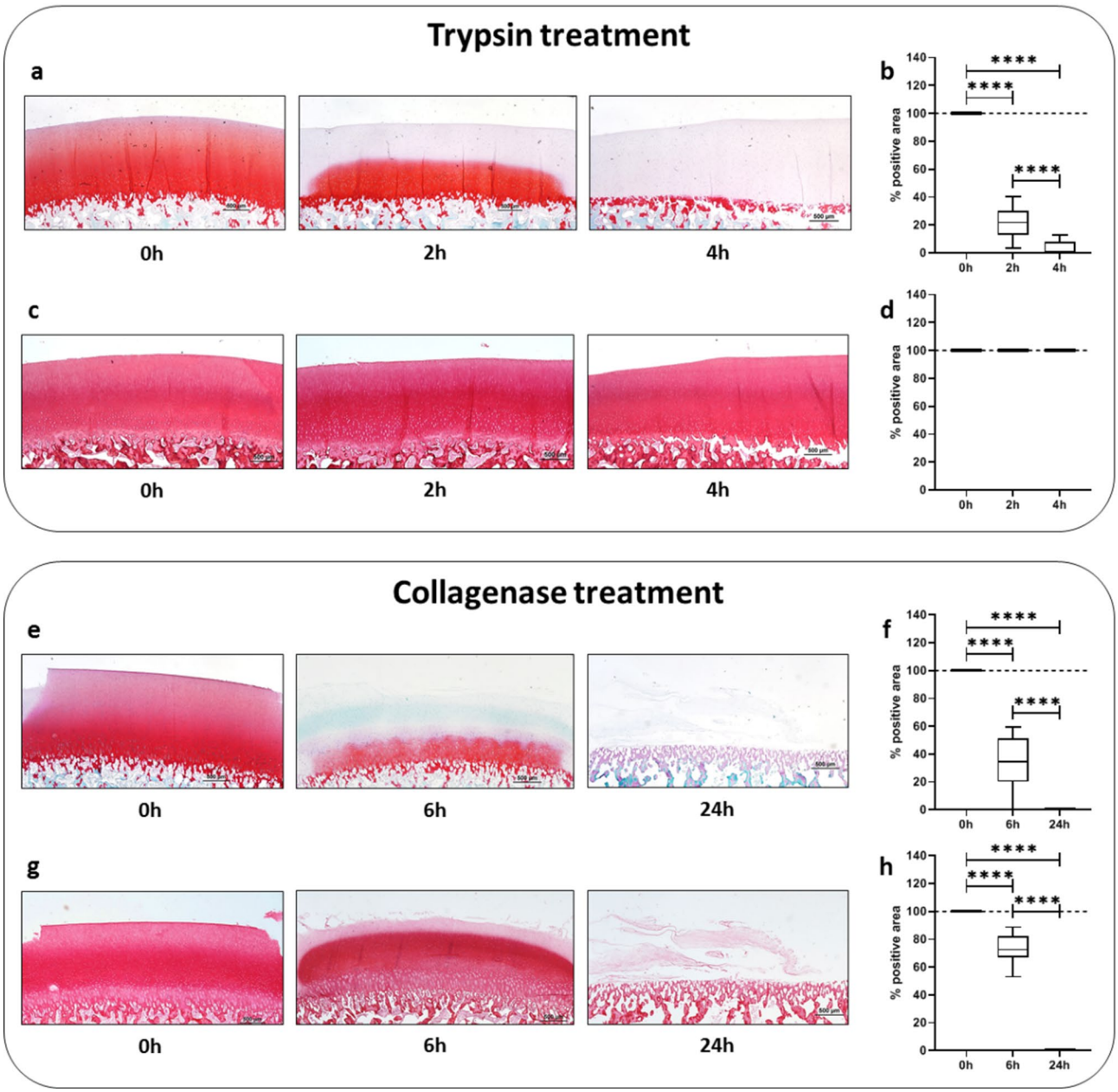


**Fig. 4**. Representative histological images of Safranin O (**a**) and Picrosirius (**c**) Red-positive stained area of the cartilage treated with trypsin at three different time points (0 h, 2 h and 4 h) with the corresponding quantification of cartilage positive area (**b**,**d**, respectively), and representative histological images of Safranin O (**e**) and Picrosirius (g) Red-positive stained area of the cartilage treated with collagenase at three different time points (0 h, 6 h and 24 h), with the corresponding quantification of cartilage positive area (**f**,**h**, respectively). Quantification of cartilage positive area (**b**,**d**,**f**,**h**) is represented as Box-plot with median, minimum and maximum. Group-wise differences were analyzed using the non-parametric Kruskal-Wallis test, with Dunn's test as a post-hoc analysis for multiple comparisons: ****$p < 0.0001$. $N = 4$ independent tissue samples per group.

tiny residual positive area (< 5%) (Fig. 4b). Quantification of Safranin O positive areas evidenced a significant decrease after trypsin treatment both at 2 h and 4 h but also between these two time points (Fig. 4b). By contrast, Picrosirius Red staining showed the preservation of collagen fibers within the cartilage even after 4 h of treatment (Fig. 4c, d), indicating that the collagen network was not affected by trypsin treatment along the cartilage thickness (100% positive staining).

*Collagenase treatment*

In the sample stained with Safranin O, collagenase treatment showed a progressive and significant decrease in proteoglycan content over time (Fig. 4e, f). The positive surface area, which corresponds to 100% of the cartilage before degradation (0 h), evidenced a significant decrease of approximately 65% after 6 h (6 h), evidencing a substantial reduction in proteoglycans and alterations of the superficial zone. On the other hand, the Picrosirius Red staining (Fig. 4g, h) also confirmed this trend, showing a reduction of collagen content from 100% at 0 h to 70% after 6 h. After 24 h (24 h) of collagenase treatment, we observed a complete depletion of the cartilage matrix. Only in a few samples, we observed the presence of the cartilage deep layer attached to the subchondral bone. Overall, the collagenase treatment significantly impacted the whole structure and thickness of the cartilage.

## AFM indentation

In Fig. 5 Young's modulus of elasticity obtained through Atomic Force Microscopy (AFM) indentation experiments are shown for cartilage before and after trypsin and collagenase treatments. The results revealed a marked decrease in the mechanical properties after both trypsin and collagenase treatments. The softening effect of collagenase treatment was particularly effective, and cartilage samples became extremely sticky after the complete depletion of collagen.

## Discussion

In this study, healthy cartilage samples were extracted from bovine condyles and subjected to enzymatic degradation using trypsin and collagenase to simulate the loss of proteoglycans and collagen networks, occurring during articular cartilage degenerative pathologies, such as OA. Three time points were established for assessing

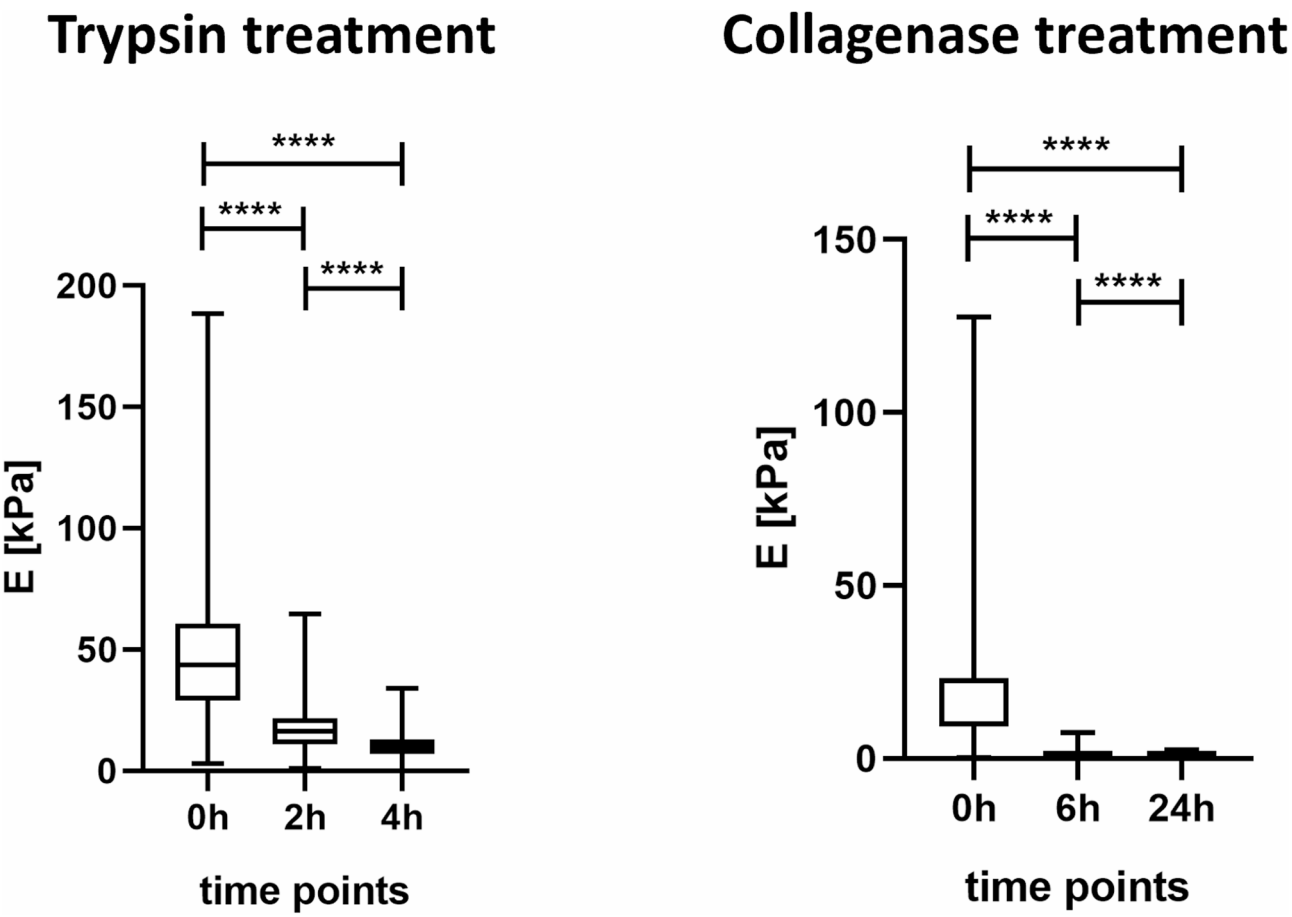


**Fig. 5**. Young's modulus of elasticity of samples treated with trypsin and collagenase, obtained through AFM indentation. Group-wise differences were analyzed using the non-parametric Kruskal-Wallis test, with Dunn's test as a post-hoc analysis for multiple comparisons: ****$p < 0.0001$. N consisted of 19 independent tissue samples per group for trypsin and 20 independent tissue samples per group for collagenase.

the outcomes of both enzymatic treatments, simulating healthy cartilage, moderate degeneration and severe degeneration.

A total of ten QUS metrics were extracted from the raw RF signals to discriminate the different degrees of degeneration induced by the two enzymes. Overall, the features varied significantly after both treatments and some metrics proved more sensitive than others in detecting even early signs of degradation (Figs. 1 and 2).

In Figs. 1a and 2a, quantitative features describing the complexity and irregularity of the time-series signals, are reported. *SampEn*, *Multiscale entropy*, and *Fuzzy entropy* have already been widely used for estimating the randomness of EEG signals[20,21] and complexity of physiological signals[22]. *Mean crossings* have found application in the joint health assessment in patients with Juvenile Idiopathic Arthritis using wearable acoustical emission measurements from the knees[23]. *Fractal dimension* has been used in previous works as a tool for analyzing the complexity of biomedical waveforms, for example in sleep electroencephalograms[24]. The potential of all these metrics for characterizing cartilage samples, based on RF data, has never been explored, except for *sampEn*, *mean crossings*, *kurtosis*, which were preliminarily investigated by the authors as a metric to discriminate between healthy and degenerated cartilage[18,25]. In this study, *sampEn*, *multiscale entropy* and *fuzzy entropy* were affected by both enzymatic treatments. They showed a slight increase following trypsin treatment, indicating greater signal randomness after proteoglycan digestion, likely due to cartilage disorganization and increased vulnerability resulting from proteoglycan loss. *SampEn*, *multiscale entropy* and *fuzzy entropy*, decreased significantly with collagenase treatment, indicating increased regularity in the time series due to the progressive degradation of the cartilage matrix. This degradation ultimately led to matrix melting and loss, reducing the inherent inhomogeneity present across its thickness[2]. Accordingly, *mean-crossings* decreased significantly after collagenase digestion, indicating a loss of signal complexity and resulting in more homogeneous time series. The *mean-crossing* results reflected the fact that the degenerative action leads to a decrease in the number of vibration patterns, which is an indicator of joint pathology[26,27]. Nevertheless, the *fractal dimension* did not reflect the reduction in time series complexity, as it remained unchanged after both treatments. *Kurtosis* also did not change after either trypsin or collagenase treatment, indicating that data distribution was unaffected by the degeneration process. Overall, these metrics were able to detect changes in the complexity and regularity of the RF signals from both healthy and chemically degraded cartilage samples. The impact of collagenase was more pronounced, leading to less complex and more regular signals following the degradation process.

Figures 1b and 2b report the results of the parameters strictly related to the structure of cartilage samples: *vii)* $RI_c$, *viii)* $RI_b$, *ix) bone propagation* and *x) cartilage length*. Ideally, we would expect $RI_c$ and *cartilage length* to decrease and $RI_b$ and *bone propagation* to increase as the degradation progresses. Indeed, as the cartilage degrades, the difference in acoustic impedance decreases at the water-cartilage interface and increases at the cartilage-bone interface. We observed no significant differences in the samples treated with trypsin, whereas samples degraded with collagenase showed a considerable and progressive decrease in $RI_c$ and *cartilage length*, resulting in a total loss of cartilage after 24 h. It was not possible to determine $RI_c$ at 24 h due to the complete absence of the water-cartilage interface. $RI_b$ showed no alteration with collagenase degradation, while *bone propagation* increased gradually, in line with the loss of the cartilage. Overall, these results revealed that collagenase had a more pronounced impact on the structure of cartilage samples compared to trypsin, in agreement with literature findings at high frequency US[8,9].

In recent years, the adoption of AI for monitoring cartilage degeneration is attracting growing interest. AI has been used for the classification of OA severity, lesion detection, cartilage segmentation, and the development of predictive models for knee OA progression[28]. Recent applications of deep learning in OA research involve the automatic detection of OA severity in radiographs and the identification of cartilage and meniscal lesions, as well as cartilage segmentation for T2 quantification in MR images. Furthermore, ML models have expanded to include the identification of individuals at high risk of developing OA using modifiable and non-modifiable risk factors such as obesity, genetic predisposition, joint injury, physical activity, and biomechanics[28]. ML models have also been developed using data from near-infrared spectroscopy to evaluate cartilage integrity during arthroscopy, enabling the distinction between healthy and diseased cartilage[29]. Moreover, in a recent study, ML and deep learning models were established by incorporating raw RF data alongside the average SoS value and T-score as QUS measurements, facilitating the creation of an in vivo automated system for osteoporosis classification and detection[30]. However, no previous ML applications have employed sets of relevant QUS features extracted from RF data to identify the degeneration status of the cartilagineous tissue.

We developed for the first time six ML models exploiting the ten relevant QUS metrics derived from RF data to automatically recognize healthy and degenerated cartilage samples. Of note, this allows an actual translational application to quantitatively assess single samples. In Figure S2, the top informative features from each QUS dataset were reported; they could serve as promising indicators for predicting individual cartilage changes through the training of ML models. Our findings demonstrate that the developed models achieved good classification accuracy in distinguishing between two degradation levels for both trypsin (60%) and collagenase treated samples (96%). However, performance declined when classifying three degradation levels, likely due to the limited size and variability of the dataset. To address this, we applied SMOTE for data augmentation, which led to a marked improvement in classification accuracy: from 41% to 93% for trypsin and from 68% to 96% for collagenase using the random forest classifier. This improvement can be attributed to the correction of class imbalance and the synthetic enrichment of the feature space. While these results are encouraging, it is important to note that SMOTE technique was applied prior to the LOOCV procedure, which may introduce overlap between training and validation sets. This overlap can lead to optimistic performance metrics due to potential data leakage. Future work will focus on applying SMOTE within each cross-validation fold to ensure a more rigorous assessment and avoid potential overfitting. Additionally, expanding the dataset with more real samples will be crucial to further validate the robustness of the classification pipeline and reduce dependency on synthetic oversampling.

Figures 4 and 5 clearly show that both trypsin and collagenase enzymes caused a progressive modification of the cartilage matrix and its mechanical properties. A significant decrease in both histological proteoglycan content and mechanical properties was found at each time point of the analysis, for both trypsin and collagenase. The histological and mechanical analyses further corroborated the findings of QUS parameters and ML classification: specifically, the impact of collagenase seemed more pronounced compared to trypsin. In particular, the trend in cartilage thickness calculated from RF data is consistent with the trend in cartilage thickness determined through histology. Trypsin had no effect on cartilage thickness since the collagen network was not affected (see Figure S1 in the supplementary material). In contrast, collagenase had a considerable impact on thickness, resulting in a significant decrease after 24 h with reductions of 75% and 54% observed through histological and US analysis, respectively (see Figure S1 in the supplementary material).

Similarly, the mechanical properties were more affected by collagenase compared to trypsin treatment. AFM results revealed a maximum decrease in the cartilage Young's modulus by 77% after 4 h of trypsin treatment. However, this change was not detected in the cartilage features, probably due to the presence of an intact collagen network, as demonstrated by the histological results. The cartilage Young's modulus decreased by 99% after 24 h of collagenase treatment. Consequently, the water-cartilage interface disappeared in the RF signal, indicating complete cartilage degradation, which made it impossible to calculate $RI_c$ after 24 h of collagenase treatment.

Although some individual metrics did not exhibit significant variations, they still contributed to the classification process (see Figure S2 of the supplementary material). Specifically, combining these QUS metrics within an optimized model enabled accurate discrimination of the degradation process. These findings suggest that QUS metrics derived from RF data, selected based on their informative weights and coupled with ML models, hold promise for the development of an automated and quantitative tool for cartilage monitoring. For a successful in vivo translation, the complexity of the biological environment must be carefully considered, as it can attenuate and distort the RF signals. To address this, a stepwise approach will be adopted for clinical implementation. Initially, RF data will be acquired from bovine cartilage explants with naturally occurring OA. Subsequently, human cartilage explants obtained from OA patients undergoing total knee replacement surgery will be analysed. Both types of samples will be scanned using the same setup and methodology described in this study. This phase will allow further refinement and optimization of the feature extraction algorithms and provide initial validation of the classification models in a more physiologically relevant context. Subsequent pilot studies will involve the acquisition of RF data directly from patients with knee OA. The resulting dataset will be labelled and used to validate both the extracted quantitative metrics and the associated algorithms. To address signal distortion caused by intervening tissues along the acoustic path, we will investigate correction strategies that include advanced signal processing techniques (e.g., adaptive filtering), calibration using tissue-mimicking phantoms[31]. Furthermore, the machine learning models must be retrained and validated with in vivo datasets to incorporate in-vivo biological information, enabling the model to adapt to more complex biological environments while maintaining accuracy and robustness.

## Conclusion

In this work, we performed a thorough analysis of radiofrequency signals acquired with an ultrasound transmission frequency equal to 15 MHz, with the aim of detecting changes in ex-vivo cartilage samples. Healthy bovine samples were enzimatically degraded using trypsin and collagenase, to simulate the loss of proteoglycans and collagen networks during degenerating pathologies, such as osteoarthritis. We extracted a total of ten quantitative ultrasound metrics, which were able to detect changes in the cartilage structure and variations in the complexity and regularity of the signals, due to the degradation process. The quantitative ultrasound metrics were used as input for machine learning models to automatically discriminate between healthy and degenerated cartilage samples. The application of the random forest model resulted in 60% classification accuracy for trypsin-treated samples, while the support vector machine achieved a notably higher accuracy of 96% in distinguishing collagenase-degraded cartilage. In general, the quantitative ultrasound metrics and classifiers performed better with the collagenase treatment; indeed, the effects on the tissue matrix were more pronounced, as confirmed by histological and mechanical findings. This work represents the first attempt to use quantitative ultrasound measures in conjunction with machine learning classifiers for assessing the cartilage status and paves the way for a future in vivo translation of this methodology. The identification of specific QUS metrics and classification methods, supported by histological and mechanical analyses, lays the groundwork for applying ultrasound technology in diagnosing cartilage defects and osteoarthritis in patients.

## Materials and methods

### Sample preparation and experimental setup

Nineteen bovine condyles, without visible lesions, were bought from a nearby market. A bone biopsy instrument was used to extract 254 samples, each with a diameter of 6 mm and a length of 5/6 mm. Healthy specimens were initially scanned with US before undergoing enzymatic degradation with trypsin ($n = 128$) and collagenase ($n = 126$). For each treatment group, 4 samples were collected for subsequent histological analysis at the 0-hour mark. The specimens of the trypsin group were immersed in a 0.25% trypsin-ethylenediamtetra-acetic acid (EDTA) (59428 C, Sigma Aldrich) solution at 37 °C, as described by Wang et *al*[8]. After 2 h and 4 h of treatment, specimens were washed in a Phosphate Buffered Saline solution (PBS, P4417, Merck) and scanned to acquire RF data. At each time point, 4 samples were sacrificed for histological analysis. The specimens of the collagenase group were placed in a 4 mg/mL collagenase solution (SCR103, Sigma Aldrich), at 37 °C[8]. After 6 h and 24 h of treatment, specimens were washed in a PBS solution and scanned to acquire RF data. At each time point, 4 samples were sacrificed for histological analysis.

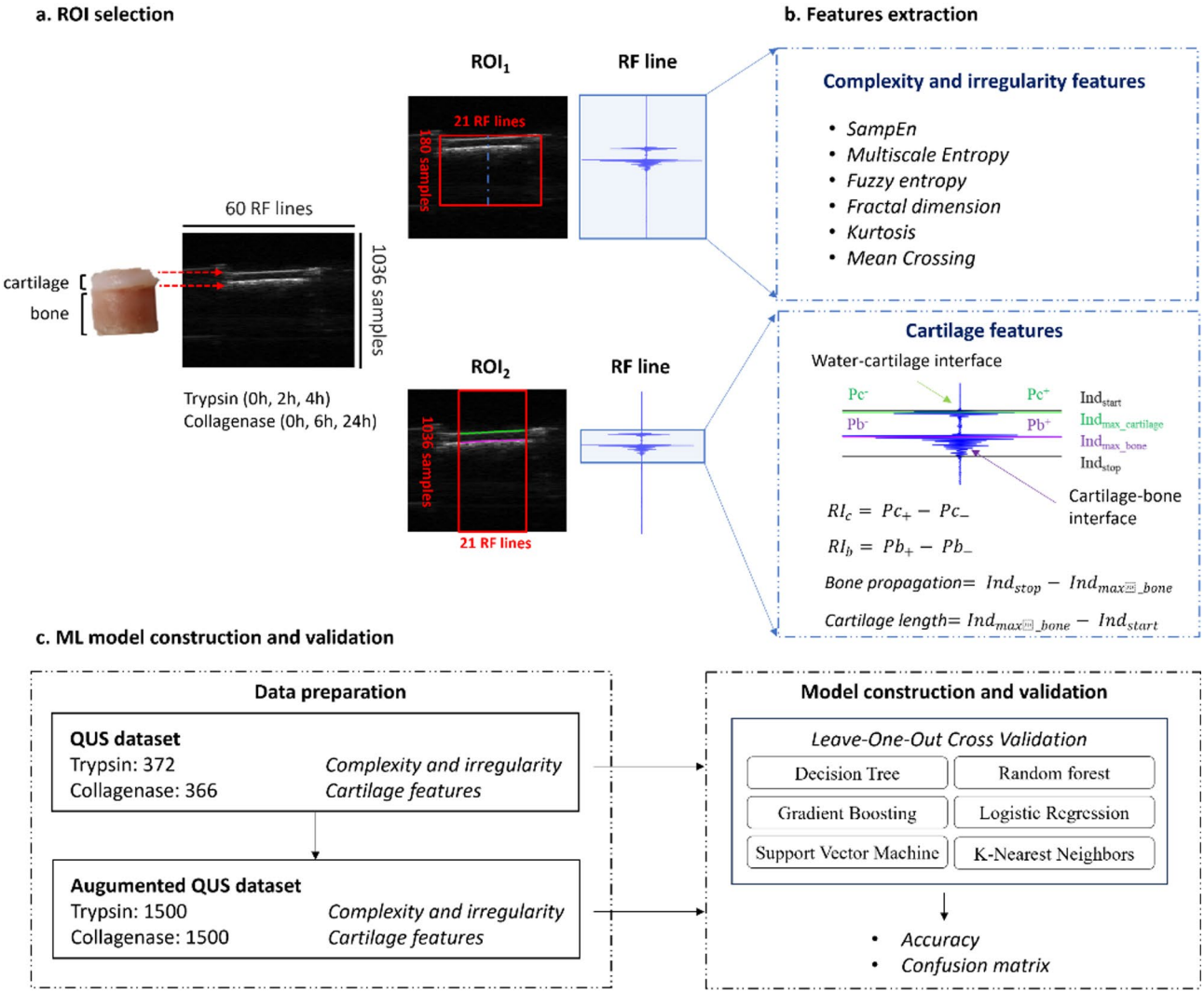


**Fig. 6**. Workflow for RF data analysis. In (**a**), a representative B-mode image is shown, highlighting the cartilage and bone interfaces. Two regions of interest were identified for feature extraction: $ROI_1$, which includes the central portion of the B-mode image and $ROI_2$, in the middle of the sample to avoid irregular boundaries. Complexity and irregularity features were calculated in $ROI_1$, while cartilage features were computed in $ROI_2$ (**b**). In (**c**), the workflow for ML model construction is represented. For each dataset (complexity and irregularity and cartilage features), a feature selection step has been applied to extract the most informative features to build the ML models.

The experimental setup used to acquire RF data is described in[17,18]. A support for the probe and a sample holder were immersed in a tank filled with deionized and degassed water. The sample holder included an agarose support with 6 mm diameter holes to host the cartilage samples. The agarose supports were prepared with a concentration of 2% w/v to prevent any interference with US beam, since it shows acoustic properties and echogenicity similar to water[32]. RF data were acquired using the ArtUS EXT-1 H system (Telemed, Italy) equipped with a 192 elements linear probe L15-7H40-A5 (7.5–15 MHz), setting the transmission frequency to 15 MHz.

In addition, a total of 49 cartilage samples were extracted from two different condyles to perform AFM analyses.

## US data analysis

A total of 738 RF acquisitions (372 for the trypsin treatment group and 366 for the collagenase treatment group consisting of 60 RF lines (columns) and 1036 samples (rows)) were processed off-line using Python and Matlab software routines. To characterize the cartilage specimens at different time points of degradation, we extracted two sets of QUS metrics for each examined RF line: complexity and irregularity metrics and cartilage features.

The complexity and irregularity metrics (*sampEn*, *multiscale entropy*, *fuzzy entropy*, *fractal dimension*, *kurtosis* and *mean crossing*) were computed within a ROI ($ROI_1$) in the central portion of the image (21 RF lines × 180 samples, see Fig. 6a, b). The cartilage features were extracted in a ROI in the middle of the sample ($ROI_2$),

where the main features are clearly visible (21 RF lines × 1036 samples, see Fig. 6a, b). They include the RI at the water-cartilage surface ($RI_c$), RI at the cartilage-bone interface ($RI_b$), *bone propagation* (indicating how much the signal is spread after the bone interface) and the *cartilage length* (calculated as the difference between the bone surface and the first signal peak). For each sample, the average value of each QUS metric was computed along the 21 RF lines.

The mathematical definition of the proposed QUS metrics is described in detail in the appendix section of the supplementary material.

*ML-based classification*

*Data.* To construct the ML models, we allocated 372 specimens (0 h: 128; 2 h: 124; 4 h: 120) from the trypsin treatment and 366 specimens (0 h: 126; 6 h: 122; 24 h: 118) from the collagenase group. For each treatment, we created two datasets: an initial training dataset (QUS dataset) with the QUS metrics and an augmented QUS dataset generated using the SMOTE technique[33], following the experimental methodology described in[34,35], to create a larger, balanced dataset with 500 samples per class. Such an augmentation provided synthetic QUS metrics, closely resembling those derived from the original specimens, allowed us to explore the potential improvement in classification accuracy when addressing class imbalance, while also evaluating the scalability of the models to larger QUS datasets.

*ML model construction and evaluation*

We conducted experiments using six well-known ML models, namely the decision tree, K-Nearest Neighbors, support vector machine, logistic regression, random forest, and Gradient Boosting, as previously studied in[36]. To assess the classifiers' ability to discriminate between different levels of degradation, we used the accuracy metric and the *confusion matrix*[28]. Accuracy reflects the proportion of correct classifications, calculated by dividing correct predictions by total predictions, while the *confusion matrix* provides a tabular report to visualize model performance against ground-truth values.

To evaluate the performance of the models to distinguish two (healthy and severe) and three levels of degeneration (healthy, moderate and severe) induced by trypsin and collagenase, we used the LOOCV technique on both original and SMOTE-augmented datasets. A graphical representation of the methodology used is provided in Fig. 6c.

## Histological analyses

Osteochondral plugs were fixed in neutral buffered formalin (10%) for 24 h, washed, placed into the decalcifying solution (MicroDecfast, Diapath S.p.A., Martinengo, BG, Italy) for 6 days, dehydrated in graded concentrations of ethanol, clarified in xilol and embedded in paraffin. As shown in supplementary Figure S3a, serial sections of 5 µm were obtained longitudinal to the osteochondral plugs in three different areas defined as α, β, and γ. Fifteen slices were obtained from each area, equally spaced from each other, to evaluate the centre of the sample. Sections were stained with Safranin O for 10 min and Fast Green for 3 min (both from Sigma Aldrich-Merck). Picrosirius Red staining was also performed using 0,1% Direct Red 80 in saturated picric acid in $H_2O$ for 60 min (Sigma Aldrich-Merck). Images were captured using an Eclipse 90i microscope (Nikon Instruments Europe BV) equipped with a CCD camera. Two independent observers selected the total cartilage area, Safranin O and Picrosirius Red positive areas of the cartilage by using the dedicated Software NIS-Elements that expressed the selected area as $\mu m^2$. As shown in supplementary Figure S3b, c, the percentage of positive area was calculated as the ratio between total and positive area[37].

## AFM indentation

AFM indentation[38] was performed employing a Nanowizard IV AFM system (Bruker, USA), mounted on a DMi8 inverted optical microscope (Leica Microsystem, Germany). Silicon nitride triangular cantilever (DNP, Bruker, USA) with a nominal spring constant of 0.24 N/m, equipped with a pyramidal probe with a typical tip radius of 20 nm was used for cartilage indentation. The actual spring constant was evaluated per each cantilever using the thermal noise method[39].

The samples were cleaned with PBS (Sigma-Aldrich, USA) and then placed in a Teflon sample holder, designed and fabricated for this purpose (see supplementary Figure S4) and filled with PBS buffer for the experiment.

Indentations were performed on untreated samples and then repeated on the same samples after the treatment with trypsin (19 samples) and collagenase (20 samples) performed in situ exploiting the custom-made Teflon holder.

Three areas of $10 \times 10$ $\mu m^2$ were tested per each sample. In each region, 400 force-distance curves[40] were acquired; in total 1200 curves per sample. The maximum force applied was 10 nN and the tip velocity was maintained at 3 µm/s.

The data were analyzed with a built-in software (Bruker, USA) using the Bilodeau formula for a regular pyramidal punch[41] that extends the Hertz-model contact mechanics to the case of non-axisymmetric indenters.

## Statistical analysis

Statistical comparisons between all experimental groups were performed using non-parametric tests, based on the non-normal distribution of histological, mechanical and RF data. Group-wise differences were analyzed using the non-parametric Kruskal-Wallis test for independent data. Dunn's test was performed as a post-hoc analysis for multiple comparisons. A p-value below the corrected significance threshold of 0.033 was considered statistically significant. All statistical analyses were conducted using GraphPad Prism (version 8.0.2).

## Data availability

The data that support the findings of this study are available from the corresponding author upon reasonable request.

Received: 18 December 2024; Accepted: 17 June 2025
Published online: 01 July 2025

## References

1. Sophia Fox, A. J., Bedi, A. & Rodeo, S. A. The basic science of articular cartilage: structure, composition, and function. *Sports Health*. **1**(6), 461–468. https://doi.org/10.1177/1941738109350438 (2009).
2. Daou, F., Cochis, A., Leigheb, M. & Rimondini, L. Current advances in the regeneration of degenerated articular cartilage: A literature review on tissue engineering and its recent clinical translation. *Materials* **15**(1), 31. https://doi.org/10.3390/ma15010031 (2021).
3. L'Hermette, M., Tourny-Chollet, C., Polle, G. & Dujardin, F. Articular cartilage, degenerative process, and repair: current progress. *Int. J. Sports Med.* **27**(9), 738–744. https://doi.org/10.1055/s-2005-872824 (2006).
4. Daher, R. J., Chahine, N. O., Greenberg, A. S., Sgaglione, N. A. & Grande, D. A. New methods to diagnose and treat cartilage degeneration. *Nat. Rev. Rheumatol.* **5**(11), 599–607. https://doi.org/10.1038/nrrheum.2009.204 (2009).
5. D'Agostino, V. et al. Ultrasound imaging in knee osteoarthritis: current role, recent advancements, and future perspectives. *J. Clin. Med.* **13**(16), 4930. https://doi.org/10.3390/jcm13164930 (2024).
6. Cloutier, G., Destrempes, F., Yu, F. & Tang, A. Quantitative ultrasound imaging of soft biological tissues: a primer for radiologists and medical physicists. *Insights Imaging*. **12**(1), 127. https://doi.org/10.1186/s13244-021-01071-w (2021).
7. Oelze, M. L. & Mamou, J. Review of quantitative ultrasound: envelope statistics and backscatter coefficient imaging and contributions to diagnostic ultrasound. *IEEE Trans. Ultrason. Ferroelectr. Freq. Control.* **63**(2), 336–351. https://doi.org/10.1109/TUFFC.2015.2513958 (2016).
8. Wang, S. Z., Huang, Y. P., Saarakkala, S. & Zheng, Y. P. Quantitative assessment of articular cartilage with morphologic, acoustic and mechanical properties obtained using high-frequency ultrasound. *Ultrasound Med. Biol.* **36**(3), 512–527. https://doi.org/10.1016/j.ultrasmedbio.2009.12.005 (2010).
9. Saarakkala, S. et al. Ultrasonic quantitation of superficial degradation of articular cartilage. *Ultrasound Med. Biol.* **30**(6), 783–792. https://doi.org/10.1016/j.ultrasmedbio.2004.03.005 (2004).
10. Wang, Q. et al. Real-Time ultrasonic assessment of progressive proteoglycan depletion in articular cartilage. *Ultrasound Med. Biol.* **34**(7), 1085–1092. https://doi.org/10.1016/j.ultrasmedbio.2007.12.006 (2008).
11. Nieminen, H. J. et al. Real-time ultrasound analysis of articular cartilage degradation in vitro. *Ultrasound Med. Biol.* **28**(4), 519–525. https://doi.org/10.1016/S0301-5629(02)00480-5 (2002).
12. Kaleva, E., Saarakkala, S., Töyräs, J., Nieminen, H. J. & Jurvelin, J. S. In-vitro comparison of time-domain, frequency-domain and wavelet ultrasound parameters in diagnostics of cartilage degeneration. *Ultrasound Med. Biol.* **34**(1), 155–159. https://doi.org/10.1016/j.ultrasmedbio.2007.06.028 (2008).
13. Lye, T. H. et al. Quantitative ultrasound assessment of early osteoarthritis in human articular cartilage using a high-frequency linear array transducer. *Ultrasound Med. Biol.* **48**(8), 1429–1440. https://doi.org/10.1016/j.ultrasmedbio.2022.03.006 (2022).
14. Niu, H. J. et al. Ultrasonic reflection coefficient and surface roughness index of OA articular cartilage: relation to pathological assessment. *BMC Musculoskelet. Disord*. https://doi.org/10.1186/1471-2474-13-34 (2012).
15. Zhang, J., Xiao, L., Tong, L., Wan, C. & Hao, Z. Quantitative evaluation of enzyme-induced porcine articular cartilage degeneration based on observation of entire cartilage layer using ultrasound. *Ultrasound Med. Biol.* **44**(4), 861–871. https://doi.org/10.1016/j.ultrasmedbio.2017.11.016 (2018).
16. Hattori, Y. T. K., Ikeuchi, K. & Morita, Y. Quantitative ultrasonic assessment for detecting microscopic cartilage damage in osteoarthritis. *Arthritis Res. Ther.* **7**(1), 1–9. https://doi.org/10.1186/ar1463 (2004).
17. Sorriento, A., Poliziani, A., Cafarelli, A., Valenza, G. & Ricotti, L. A novel quantitative and reference-free ultrasound analysis to discriminate different concentrations of bone mineral content. *Sci. Rep.* **11**(1), 1–14. https://doi.org/10.1038/s41598-020-79365-0 (2021).
18. Sorriento, A., Cafarelli, A., Valenza, G. & Ricotti, L. Ex-vivo quantitative ultrasound assessment of cartilage degeneration. In *Annu. Int. Conf. IEEE Eng. Med. Biol. Soc.* 2976–2980. https://doi.org/10.1109/EMBC46164.2021.9630198 (2021).
19. Bradshaw, T. J., Huemann, Z., Hu, J. & Rahmim, A. A guide to cross-validation for artificial intelligence in medical imaging. *Radiol. Artif. Intell.* https://doi.org/10.1148/ryai.220232 (2023).
20. Wang, H. et al. Driving fatigue classification based on fusion entropy analysis combining EOG and EEG. *IEEE Access.* **7**, 61975–61986. https://doi.org/10.1109/ACCESS.2019.2915533 (2019).
21. Ji, M., Zhang, E. E. G. & Dong, and Signals feature extraction based on DWT and EMD combined with approximate entropy. *Brain Sci.* **9**(8), 201. https://doi.org/10.3390/brainsci9080201 (2019).
22. Azami, H., Li, P., Arnold, S. E., Escudero, J. & Humeau-Heurtier, A. Fuzzy entropy metrics for the analysis of biomedical signals: assessment and comparison. *IEEE Access.* **7**, 104833–104847. https://doi.org/10.1109/ACCESS.2019.2930625 (2019).
23. Semiz, B. et al. Using knee acoustical emissions for sensing joint health in patients with juvenile idiopathic arthritis: A pilot study. *IEEE Sens. J.* **18**(22), 9128–9136. https://doi.org/10.1109/JSEN.2018.2869990 (2018).
24. Raghavendra, B. S. & Narayana Dutt, D. A note on fractal dimensions of biomedical waveforms. *Comput. Biol. Med.* **39**(11), 1006–1012. https://doi.org/10.1016/j.compbiomed.2009.08.001 (2009).
25. Guachi-Guachi, L. et al. Quantitative ultrasound assessment of healthy and degenerated cartilage. In *2023 IEEE International Ultrasonics Symposium (IUS)*, 1–4 https://doi.org/10.1109/IUS51837.2023.10306623 ( IEEE, 2023).
26. Whittingslow, D. C. et al. Knee acoustic emissions as a digital biomarker of disease status in juvenile idiopathic arthritis. *Front. Digit. Health*. https://doi.org/10.3389/fdgth.2020.571839 (2020).
27. Karpiński, R. et al. Diagnostics of articular cartilage damage based on generated acoustic signals using ANN—Part II: patellofemoral joint. *Sensors* **22**(10), 3765. https://doi.org/10.3390/s22103765 (2022).
28. Joseph, G. B. et al. AI MSK clinical applications: cartilage and osteoarthritis. *Skeletal Radiol.* **51**(2), 331–343. https://doi.org/10.1007/s00256-021-03909-2 (2022).
29. Afara, I. O. et al. Machine learning classification of articular cartilage integrity using near infrared spectroscopy. *Cell. Mol. Bioeng.* **13**(3), 219–228. https://doi.org/10.1007/s12195-020-00612-5 (2020).
30. Luo, W. et al. Osteoporosis diagnostic model using a multichannel convolutional neural network based on quantitative ultrasound radiofrequency signal. *Ultrasound Med. Biol.* **48**(8), 1590–1601. https://doi.org/10.1016/j.ultrasmedbio.2022.04.005 (2022).
31. McGarry, C. K. et al. Tissue mimicking materials for imaging and therapy phantoms: a review. *Phys. Med. Biol.* https://doi.org/10.1088/1361-6560/abbd17 (2020).
32. Cafarelli, A. et al. Tuning acoustic and mechanical properties of materials for ultrasound phantoms and smart substrates for cell cultures. *Acta Biomater.* https://doi.org/10.1016/j.actbio.2016.11.049 (2017).
33. Chawla, N. V., Bowyer, K. W., Hall, L. O. & Kegelmeyer, W. P. SMOTE: synthetic minority over-sampling technique. *J. Artif. Intell. Res.* **16**, 321–357. https://doi.org/10.1613/jair.953 (2002).

34. García, V., Sánchez, J. S. & Mollineda, R. A. Exploring the performance of resampling strategies for the class imbalance problem. 541–549. https://doi.org/10.1007/978-3-642-13022-9_54 (2010).
35. Raghuwanshi, B. S. & Shukla, S. SMOTE based class-specific extreme learning machine for imbalanced learning. *Knowl. Based Syst.* **187**, 104814. https://doi.org/10.1016/j.knosys.2019.06.022 (2020).
36. Mahesh, B. Machine learning algorithms-a review. *Int. J. Sci. Res. (IJSR).* **9**(1), 381–386. https://doi.org/10.21275/ART20203995 (2020).
37. Qin, L. et al. Ultrasound detection of trypsin-treated articular cartilage: its association with cartilaginous proteoglycans assessed by histological and biochemical methods. *J. Bone Min. Metab.* **20**(5), 281–287. https://doi.org/10.1007/s007740200040 (2002).
38. Kerdegari, S. et al. Insights in cell biomechanics through atomic force microscopy. *Materials* **16**(8), 2980. https://doi.org/10.3390/ma16082980 (2023).
39. Hutter, J. L. & Bechhoefer, J. Calibration of atomic-force microscope tips. *Rev. Sci. Instrum.* **64**(7), 1868–1873. https://doi.org/10.1063/1.1143970 (1993).
40. Cappella, B., Baschieri, P., Frediani, C., Miccoli, P. & Ascoli, C. Force-distance curves by AFM. *IEEE Eng. Med. Biol. Mag.* **16**(2), 58–65. https://doi.org/10.1109/51.582177 (1997).
41. Bilodeau, G. G. Regular pyramid punch problem. *J. Appl. Mech.* **59**(3), 519–523. https://doi.org/10.1115/1.2893754 (1992).


## Acknowledgements

This work received funding from the European Union's Horizon 2020 research and innovation program, grant agreement No 814413, project ADMAIORA (ADvanced nanocomposite MAterIals fOr in situ treatment and ultRAsound-mediated management of osteoarthritis). We also acknowledge the support of the BRIEF "Biorobotics Research and Innovation Engineering Facilities" (project identification code IR0000036), project funded under the National Recovery and Resilience Plan (NRRP), Mission 4 Component 2 Investment 3.1 of Italian Ministry of University and Research funded by the European Union – NextGenerationEU. The authors would like to express their great appreciation to Angelo, from the Antica Macelleria Cafarelli, for providing us with the ex-vivo samples.

## Author contributions

A.C., L.R. and A.S. conceived and designed the study. A.S. led the experimental work. A.S. and C.T. prepared the cartilage samples and conducted the ultrasound acquisitions. E.L., P.D. and G.L. carried out histological analyses. S.K. and C.C. performed AFM indentation. A.S., L.G. and G.V. analysed ultrasound data and performed statistical evaluations. A.C. supervised the data analysis and contributed to data interpretation. A.S. and L.G. wrote the manuscript. All the authors reviewed the manuscript. L.R. secured funding for this study.

## Declarations

## Competing interests

The authors declare no competing interests.

## Additional information

**Supplementary Information** The online version contains supplementary material available at https://doi.org/10.1038/s41598-025-07827-4.

**Correspondence** and requests for materials should be addressed to A.S.

**Reprints and permissions information** is available at www.nature.com/reprints.

**Publisher's note** Springer Nature remains neutral with regard to jurisdictional claims in published maps and institutional affiliations.